

# Digital Charge Balance Controller with Low Gate Count to Improve the Transient Response of Buck Converters

Eric Meyer

Student Member, IEEE  
Queen's University  
Kingston, ON, Canada  
eric.meyer@ece.queensu.ca

Zhiliang Zhang

Member, IEEE  
Aero-Power Sci-Tech Center  
Nanjing University of Aeronautics and  
Astronautics, Nanjing, China  
zlzhang@nuaa.edu.cn

Yan-Fei Liu

Senior Member, IEEE  
Queen's University  
Kingston, ON, Canada  
yanfei.liu@queensu.ca

**Abstract** -- A linear/non-linear digital controller is presented which allows a Buck converter to recover from a load transient event with near-optimal voltage deviation and recovery time. It is demonstrated that near-optimal transient performance can be obtained without information pertaining to the Buck converter's output inductor. The proposed controller can also be extended to applications which require load-line regulation. Unlike previous digital time-optimal controllers, the proposed controller does not require digital multiplier or divider blocks nor does it require two-dimensional look-up tables. Thus, the controller can be implemented with a significantly low gate count allowing for the use of low-cost FPGAs or CPLDs. Furthermore, the proposed controller provides an excellent transient response as it is capable of reacting asynchronously to a load transient event.

**Index Terms**--DC-DC power conversion, Digital Control, Time Optimal Control, Transient Response

## I. INTRODUCTION

Considerable research has been conducted in non-linear and linear/non-linear controllers which are capable of minimizing the voltage deviation and recovery time of a DC-DC converter undergoing a load transient event. Such control methods are often referred to as "optimal control".

In [1]-[2], a non-linear analog controller is presented which employs a second-order curved switching surface to control the switching action of a Buck converter. While a near-optimal transient response is observed, the use of an analog multiplier/divider circuit significantly increases the cost and decreases the maximum switching frequency of the controller. In [3], a linear/non-linear analog controller is presented which drives a Buck converter to recovery in near-minimum time through determination of capacitor charge regions during a load transient event. The controller only employs simple mathematical functions (integration, subtraction, addition) to determine optimal switching times; however, it requires a high-speed quasi-differentiator to detect the capacitor current zero cross-over point. Furthermore, the control method is not compatible with high-performance digital features.

Digital control has gained popularity due to its unique characteristics such as robustness and re-programmability along with its ability to employ such features as parameter auto-tuning and online efficiency optimization. Thus,

numerous digital linear/non-linear optimal control methods have been researched [4]-[9]. In [4], the concept of optimal control is demonstrated experimentally by calculating the optimal switching paths for a variety of transient conditions and programming them into a digital controller. However, the controller only functions in open-loop configuration; thus, the magnitude and time instant of a transient event must be pre-defined. In [5]-[9], digital optimal control schemes are discussed which are able to drive a Buck converter to recovery in near-optimal time "on-the-fly". The controllers in [5]-[9] suffer from at least one of the following drawbacks:

- 1) Slow reaction to load transient events (either due to synchronous sampling delay or loose transient detection thresholds) which result in sub-optimal voltage deviations and recovery times [5]-[8].
- 2) Complex mathematical functions (e.g. multiplication/division/square-root) are performed requiring either slow digital multipliers or numerous large two-dimensional look-up tables (LUTs) [5]-[9].
- 3) Nominal inductor value must be known to perform switching interval calculations [5]-[8].
- 4) No extension for load-line regulation (a.k.a. adaptive voltage positioning AVP) applications have been presented [6]-[8].

In this paper a digital charge balance controller is presented which addresses and corrects the above drawbacks. Section II will outline the basic operation of the proposed controller. Section III demonstrates how capacitor charge balance integral regions can be calculated using a digital double accumulator. Section IV provides detailed operation of the controller following a load transient. Experimental results demonstrating the effectiveness of the controller are presented in Section V.

## II. BASIC CONCEPT OF OPERATION

This section will describe the high-level operation of the proposed digital charge balance controller. Fig. 1 illustrates the block diagram of a single phase synchronous Buck converter and the proposed controller. The controller's transient response will be described without and with load-line regulation.

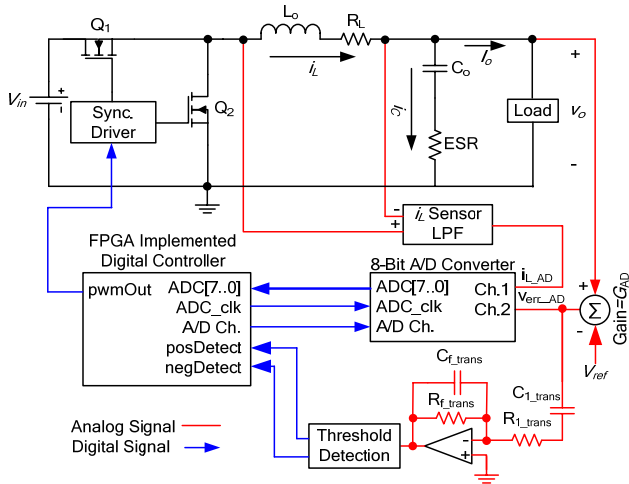


Fig. 1. Block diagram of Buck converter and proposed controller

### A. Without Load-Line Regulation

Fig. 2 and Fig. 3 show the transient reaction of a Buck converter, controlled by the proposed method, undergoing a positive and negative load step respectively.

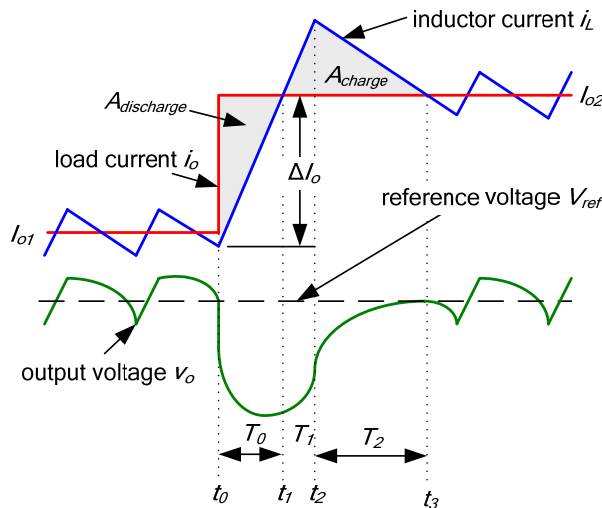


Fig. 2. Proposed controller operation following a positive load step

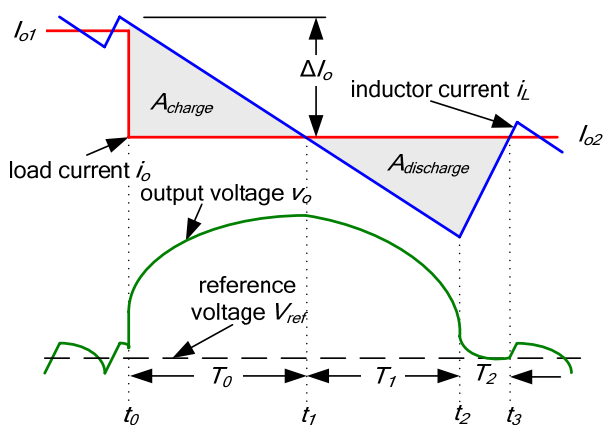


Fig. 3. Proposed controller operation following a negative load step

The key points of the controller can be summarized in three steps:

- 1) The converter is controlled by a linear voltage-mode control scheme during steady-state conditions.
- 2) Immediately following a load step change, the controller sets the PWM control high (for a positive load step change) or low (for a negative load step change).
- 3) The controller will set the PWM low (for a positive load step) or high (for a negative load step) at a determined switching time instant  $t_2$ .  $t_2$  should be such that the net capacitor charge over the transient period is zero (i.e.  $A_{charge} = A_{discharge}$ ). This will cause the output voltage to equal the reference voltage at the exact moment that the inductor current equals the load current. Determination of  $t_2$  will be discussed in Section III.

Following the recovery from the load transient, the controller will return to its linear voltage-mode operation.

### B. With Load-Line Regulation

Load-line regulation (a.k.a. adaptive voltage positioning AVP) has increasingly become a requirement in many Buck converter applications. Load-line regulation essentially involves outputting lower voltages during higher load current conditions. This assists in improving the overall transient performance of the converter along with decreasing power consumption of the load device. As will be demonstrated, the proposed controller is capable of smoothly transitioning between two steady-state voltages in order to facilitate load-line regulation. In order to describe the operation of the digital charge balance controller with load-line regulation, two separate cases must be taken into consideration.

#### 1) Case #1

As illustrated in Fig. 4, Case #1 occurs when the voltage deviation magnitude is larger than the allowed steady-state voltage change (determined by the droop resistance

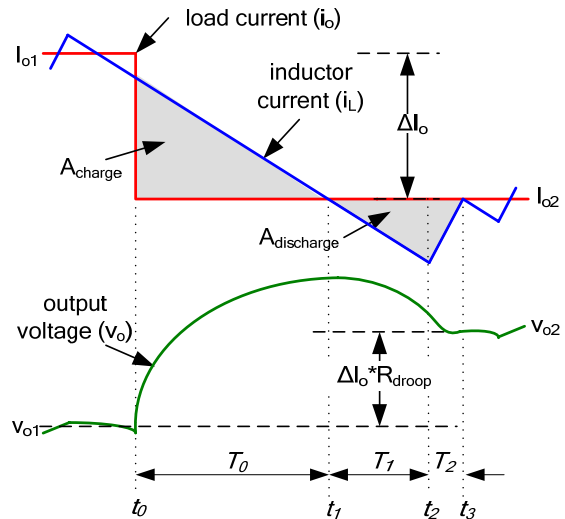


Fig. 4. Proposed controller operation following a negative load step (with load-line regulation Case #1)

$|v_{o2}-v_{o1}|$ ), as expressed in the following relation (1).

$$\frac{\left| \int_{t_0}^{t_1} (i_L - i_o) dt \right|}{C_o} \geq |\Delta I_o| \cdot R_{droop} \quad (1)$$

$t_1$  represents the first instance that the inductor current  $i_L$  equals the new load current  $I_{o2}$ . The constant  $R_{droop}$  represents the Buck converter's desired output impedance.  $\Delta I_o$  represents the difference between the final load current  $I_{o2}$  and the initial load current  $I_{o1}$ .  $C_o$  equals the Buck converter's output capacitance. For a negative load step, under Case #1 conditions, the PWM signal will be kept low from  $t_0$  to  $t_2$ .  $t_2$  is such that (2) is true. For a positive load step, under Case #1 conditions, the PWM signal will be kept high from  $t_0$  to  $t_2$ .  $t_2$  is such that (3) is true. Determination of  $t_2$  will be discussed in Section III.

$$A_{discharge} - A_{charge} = \Delta I_o \cdot R_{droop} \cdot C_o \quad (2)$$

$$A_{charge} - A_{discharge} = -\Delta I_o \cdot R_{droop} \cdot C_o \quad (3)$$

It is important to note that for low duty-cycle applications (eg. 12VDC $\rightarrow$ 1.5VDC conversion), Case #1 will likely occur for negative load current step changes since it is common practice to allow the output voltage to overshoot the load-line regulation window for a short period of time.

### 2) Case #2

Case #2 occurs when the output voltage deviation magnitude (at  $t_1$ ) is less than the allowed steady-state voltage change, (determined by droop resistance  $|v_{o1}-v_{o2}|$ ), as shown in Fig. 5 for a positive load current step change.

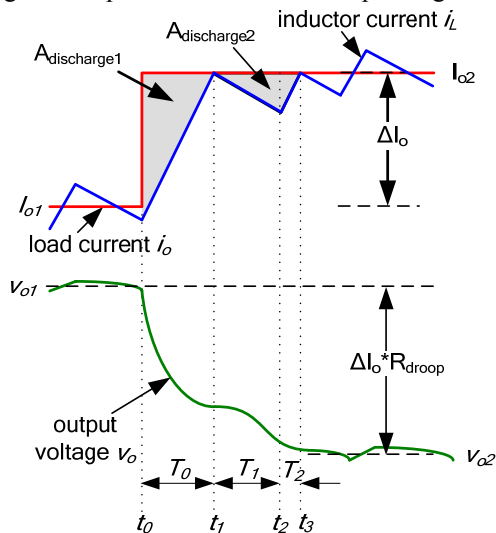


Fig. 5. Proposed controller operation following a positive load step (with load-line regulation Case #2)

It is observed that an additional switching instant must occur in order to allow the output voltage to reach the new steady state-state value with minimal settling time. At time instant  $t_1$  (the moment that the inductor current first equals the new load current), the PWM signal is set low in order to remove additional charge from the capacitor. At time instant  $t_2$ , the PWM signal is set high such that at  $t_3$ , the inductor

current equals the new load current and (4) is true.

$$A_{discharge1} + A_{discharge2} = \Delta I_o \cdot R_{droop} \cdot C_o \quad (4)$$

For low duty-cycle applications (e.g. 12VDC $\rightarrow$ 1.5VDC conversion), Case #2 will likely occur for positive load step changes since it is common practice to design the load-line regulation voltage window based on the worst case transient conditions (i.e. unloading transient events). Determination of  $t_2$  will be discussed in Section III.

## III. CALCULATION OF SWITCHING INTERVALS BASED ON A DIGITAL DOUBLE ACCUMULATOR

This section will highlight the use of a digital double accumulator to determine the switching instant  $t_2$  required such that  $A_{charge}$  and  $A_{discharge}$  are balanced appropriately.

### A. Without Load-Line Regulation

Referring to Fig. 2-Fig. 5, it is the calculation of the switching point  $t_2$  that typically requires complex mathematical computation in [5]-[9]. However, it is demonstrated in [3] that through the use of a double integrator, the switching point  $t_2$  may be determined in real-time without the use of multiplication/division. The charge balance equations, previously derived in [3], are expressed in (5) and (6) for a positive and negative load step respectively.

$$V_o \iint_{t_0}^{t_1} dt dt - V_{in} \iint_{t_1}^{t_2} dt dt = 0 \quad (5)$$

$$(V_{in} - V_o) \iint_{t_0}^{t_1} dt dt - V_{in} \iint_{t_1}^{t_2} dt dt = 0 \quad (6)$$

Thus, a digital double accumulator (see Fig. 6) may be employed (in lieu of an analog double integrator) to calculate the optimal switching moment  $t_2$ , as illustrated in Fig. 7.

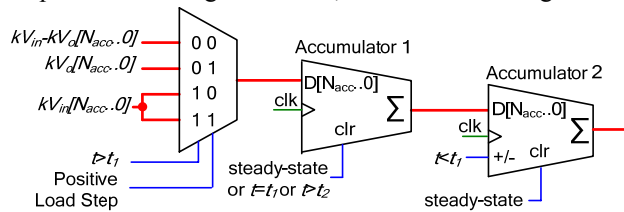


Fig. 6. Simplified diagram of digital double accumulator

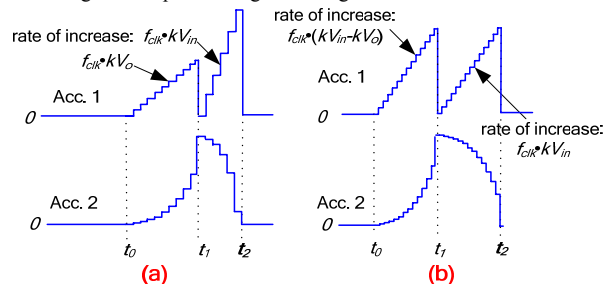


Fig. 7. Double accumulator operation: a) during positive load step, b) during negative load step

$kV_{in}$  and  $kV_o$  are digital variables representing the input and output voltage of the Buck converter.  $f_{clk}$  represents the clock frequency of the double accumulator. The input voltage

of the converter may be pre-programmed or sensed using a slow analog-digital converter. As illustrated, the switching moment  $t_2$  is determined when the double accumulator output returns to zero. However, modifications must be made to this method for applications which require load-line regulation.

### B. With Load-Line Regulation

This analysis will be separated into Case #1 and Case #2, as defined in Section II.

#### 1) Case #1

Referring to Fig. 4, the controller's goal is to drive the converter such that the inductor current reaches the new load current at the exact moment ( $t_3$ ) that the output voltage reaches its new steady state voltage  $v_{o2}$ .

In order to achieve this, equation (3) is modified such that  $A_{charge}$  and  $A_{discharge}$  are expressed in terms of the positive and negative slew rates of the inductor current, as shown in (7).

$$\int_{t_0}^{t_1} m_2 dt dt - \int_{t_1}^{t_2} \frac{m_1 \cdot m_2 - m_2^2}{m_1} dt dt = -\Delta I \cdot R_{droop} \cdot C_o \quad (7)$$

$m_1$  represents the positive slew rate of the inductor current when the converter's PWM signal is high.  $m_2$  represents the negative slew rate of the inductor current when the converter's PWM signal is low. By assuming that the load current step magnitude is large compared to the magnitude of the steady-state capacitor ripple current,  $\Delta I_o$  can be estimated by integrating the negative inductor current slew rate  $m_2$  over the time period  $T_0$  (from  $t_0$  to  $t_1$ ), as shown in (8).

$$\int_{t_0}^{t_1} m_2 dt dt - \int_{t_1}^{t_2} \frac{m_1 \cdot m_2 - m_2^2}{m_1} dt dt = R_{droop} \cdot C_o \int_{t_0}^{t_1} m_2 dt \quad (8)$$

$m_2$  can be divided from all terms of (8). The approximations  $m_1 = (V_{in} - V_o)/L_o$  and  $m_2 = -V_o/L_o$  are then substituted into (8) to produce (9).

$$\int_{t_0}^{t_1} dt dt - \int_{t_1}^{t_2} \frac{V_{in} - V_o - (-V_o)}{\frac{V_{in} - V_o}{L}} dt dt = R_{droop} \cdot C_o \int_{t_0}^{t_1} dt \quad (9)$$

By simplifying (9) and multiplying both sides of the equation by  $(V_{in} - V_o)$ , the final equation is presented in (10).

$$(V_{in} - V_o) \int_{t_0}^{t_1} dt dt - V_{in} \int_{t_1}^{t_2} dt dt = R_{droop} \cdot C_o \cdot (V_{in} - V_o) \int_{t_0}^{t_1} dt \quad (10)$$

Thus,  $t_2$  can be determined for a negative load current step change, with load line regulation implemented, by using the digital accumulator operation illustrated in Fig. 8.

It is observed that an additional digital accumulator (*load-line accumulator*) is required when load line regulation is enabled. For a negative load step,  $C_o \cdot R_{droop} \cdot f_{clk} \cdot (kV_{in} - kV_o)$  is applied to input of the *load-line accumulator* for the interval  $T_0$  (from  $t_0$  to  $t_1$ ), according to (10).

Essentially, the charge balance "zero" of the second accumulator is shifted to compensate for load line regulation. It should be noted that the output of a single accumulator is

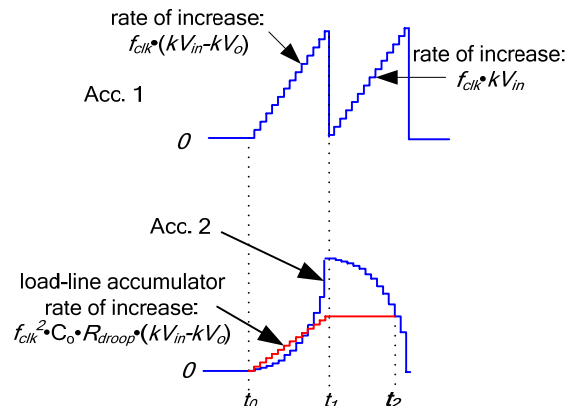


Fig. 8. Digital double accumulator operation for negative load current step with load line regulation (Case #1)

being compared to the output of two accumulators in series; therefore, the input constant ( $R_{droop} \cdot C_o$ ) of the load-line accumulator must be multiplied by  $f_{clk}$ .

If at  $t_1$ , the value of the load-line accumulator is greater than that of *accumulator 2*, inequality (1) is not satisfied, and Case #2 is detected.

#### 2) Case #2

Referring to Fig. 5, the positive load step change will be used as an example since Case #2 is not as likely to occur for a negative load step. The charge balance formula can be calculated using (11).

$$A_{discharge1} + A_{discharge2} = \Delta I \cdot R_{droop} \cdot C_o \quad (11)$$

Through similar derivation as presented above, equation (11) can be modified to (12).

$$\int_{t_0}^{t_1} m_1 dt dt + \int_{t_1}^{t_2} \frac{m_1 \cdot m_2 - m_2^2}{m_1} dt dt = R_{droop} \cdot C_o \int_{t_0}^{t_1} m_1 dt \quad (12)$$

Equation (12) can be simplified by first multiplying both sides of the equation by  $(m_2/m_1)$ , as expressed in (13).

$$\int_{t_0}^{t_1} m_2 dt dt + \int_{t_1}^{t_2} \frac{m_2^2}{m_1^2} \cdot (m_1 - m_2) dt dt = R_{droop} \cdot C_o \int_{t_0}^{t_1} m_2 dt \quad (13)$$

Since  $m_2$  and  $m_1$  are assumed to be constant, the second double integration term can be simplified by modifying the period of integration, as expressed in (14).

$$\int_{t_0}^{t_1} m_2 dt dt + \int_{\frac{|m_2|}{m_1} T_1}^{t_2} (m_1 - m_2) dt dt = R_{droop} \cdot C_o \int_{t_0}^{t_1} m_2 dt \quad (14)$$

$T_0$  and  $T_1$  are switching intervals, as shown in Fig. 5. Equation (14) implies that at the moment that the output of *accumulator 2* equals that of the load-line accumulator, the time interval is  $|m_2/m_1|$  of  $T_1$ . It is now necessary to determine time interval  $T_1$  (and thus switching time instant  $t_2$ ). Using the mathematical relationship (15), an additional accumulator (*Case 2 accumulator*) can be used to determine  $T_1$ .

$$\int_{\frac{|m_2|}{|m_1|} \cdot T_1}^{|m_2| \cdot T_1} |m_1| dt - \int_{T_1}^{|m_2| \cdot T_1} |m_2| dt = 0 \quad (15)$$

By simplifying (15), substituting in for  $m_1$  and  $m_2$  and multiplying both sides by  $L_o$ , equation (16) is created.

$$\int_{\frac{|m_2|}{|m_1|} \cdot T_1}^{|m_2| \cdot T_1} (V_{in} - 2 \cdot V_o) dt - \int_{\frac{|m_2|}{|m_2|} \cdot T_1}^{|m_2| \cdot T_1} V_o dt = 0 \quad (16)$$

Therefore, through use of an additional accumulator and the relationship (16), it is possible to determine  $t_2$ , as illustrated in Fig. 9. It is noted that no multipliers or 2-dimensional LUTs were required to calculate  $t_2$ .

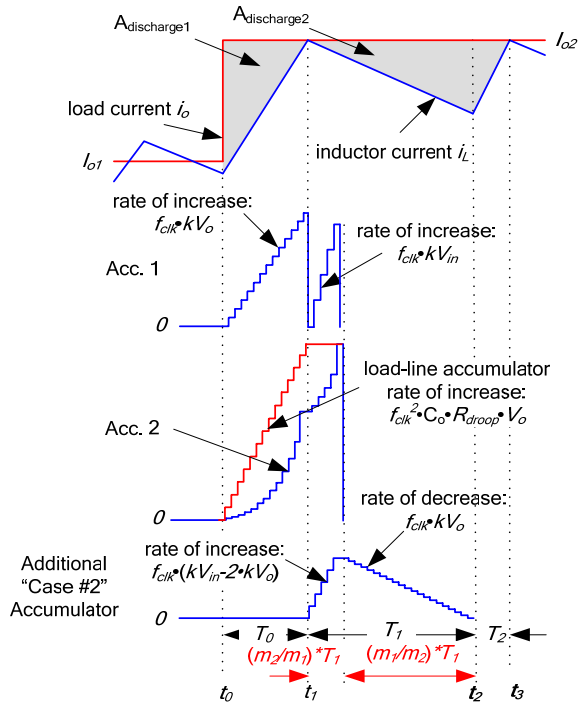


Fig. 9. Digital double accumulator operation for positive load step with load line regulation (Case #2)

#### IV. DETAILED OPERATION OF DIGITAL CHARGE BALANCE CONTROLLER

During steady-state conditions, the converter is controlled by a digital linear voltage-mode compensator. In order to implement steady-state load-line regulation, the compensator's digital error input is shifted based on measured inductor current values. In order to prevent significant loop interaction between the voltage-loop and the load-line loop, the steady-state controller calculates the load current by averaging the inductor current of four successive switching periods.

As shown in Fig. 1, the analog voltage error is fed to the ADC and to a quasi-differentiator (with roughly the same time constant as the  $C_o/ESR$  combination of the converter's output capacitor). Following a load transient, the output of

the quasi-differentiator will rapidly exceed a pre-determined threshold causing either the *posDetect* or *negDetect* signal to go high. The pre-determined threshold should be such that it is only exceeded during large load transients. The detection of either signal will cause the controller to immediately enter transient mode. At this point, the linear controller integration will be frozen and the charge balance controller will retain control of the converter. The operation of the charge balance controller can be described in four steps.

##### A. Step 1: Detect Load Transient and React

Following the detection of a load transient (at  $t_0$ ), the converter's PWM signal will be controlled by the charge balance controller. For a positive load step, the PWM control of the converter will be initially set high. For a negative load step, the PWM control will be initially set low.

The 4:1 input MUX (see Fig. 6) will select either  $kV_o$  (for a positive load step) or  $kV_{in} - kV_o$  (for a negative load step). The output of *accumulator 1* will begin to increase linearly and the output of *accumulator 2* will begin to increase exponentially. If load-line regulation is enabled, the *load-line accumulator's* output will begin to increase linearly at a rate of  $f_{clk}^2 \cdot R_{droop} \cdot C_o \cdot (kV_{in} - kV_o)$  (for a negative load current step) or  $f_{clk}^2 \cdot R_{droop} \cdot C_o \cdot kV_o$  (for a positive load current step).

##### B. Step 2: Predict Capacitor Current Zero-Crossover Point

It is crucial to precisely determine the capacitor current zero cross-over point ( $t_1$ ). In order to estimate the capacitor current, it is possible to approximate the output voltage derivative by over-sampling ( $f_{samp} \gg f_{sw}$ ) the voltage error and measuring the difference between successive samples. However, since it is important to determine the precise time instant  $t_1$ , it is necessary to detect  $t_1$  with fine resolution. By increasing the sampling frequency, the time resolution of  $t_1$  can be improved; however, quantization noise will be increased. In addition, since the output voltage is relatively flat for a substantial period before and after the capacitor current zero cross-over point, it is difficult to accurately determine the precise moment that the output voltage derivative changes signs through direct digital sampling.

Thus, in order to improve the effective resolution and accuracy of  $t_1$  while not excessively increasing the sampling frequency, a zero cross-over point predictor is proposed, as shown in Fig. 10. The predictor is similar to the hybrid capacitor current estimator presented in [8]; however in the proposed method, the inductor value is not required. As shown in Fig. 10, the voltage error derivative is monitored for a set interval following the load step. The concept of the  $i_c$  zero cross-over predictor consists of two points: a) calculate the absolute value of the slope of the voltage error derivative over the monitoring period, b) calculate the magnitude of the voltage error derivative at  $n=k_{end}$ .

The absolute value of the slope is calculated by comparing the voltage error derivative at the end of the monitoring

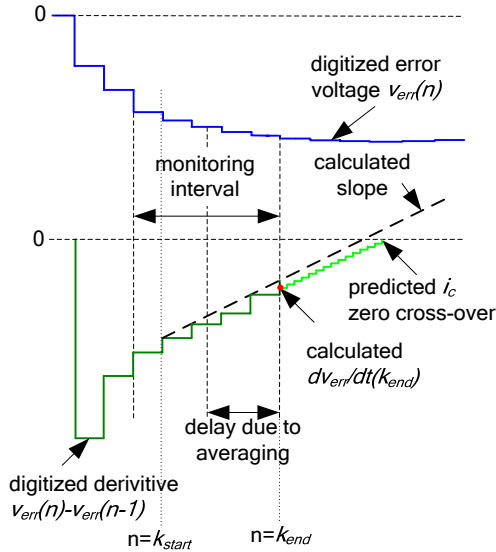


Fig. 10. Concept of capacitor current zero cross-over point prediction period to the voltage error derivative at the beginning of the monitoring period, as equated in (17).

$$|m_{ic}| = \left| \frac{dv_{err}}{dt}(k_{start}) - \frac{dv_{err}}{dt}(k_{end}) \right| \quad (17)$$

The magnitude of the output voltage derivative at  $k_{end}$  can be estimated by calculating the average of successive derivative samples and then adding a term to compensate for the averaging and ADC acquisition delay, as equated in (18).

$$|i_c(k_{end})| = \frac{T_{ic\_acq}}{T_{ic\_clk}} \left[ \sum_{n=k_{start}+1}^{n=k_{end}} \frac{dv_{err}}{dt}(n) \right] + \frac{|m_{ic}|}{2} \cdot \left( N_{samp} + 1 \right) + \frac{T_{AD\_del}}{T_{ic\_acq}} |m_{ic}| \quad (18)$$

$T_{ic\_clk}$  equals the effective timing resolution of the  $i_c$  zero crossover predictor which is determined by the system clock frequency.  $T_{ic\_acq}$  is equal to the period at which the voltage error derivative is being calculated.  $N_{samp}$  equals the number of  $T_{ic\_acq}$  periods that occur in the monitoring period (e.g. In the case of Fig. 10,  $N_{samp} = 4$ ).  $T_{AD\_del}$  equals the ADC delay. For relatively simple digital calculation,  $N_{samp}$  and  $T_{ic\_acq}/T_{ic\_clk}$  should be chosen to be  $2^x$ . In this manner, multiplication can be carried out by simply shifting register bits. Using the capacitor current slope and magnitude calculated in (17) and (18) respectively, it is possible to predict  $t_1$ , by use of an accumulator as illustrated in Fig. 11.

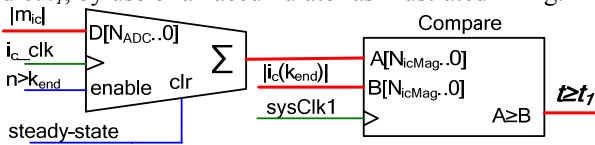


Fig. 11. Accumulator setup to predict capacitor zero cross-over point  $t_1$

After the monitoring interval, the accumulator output will increase linearly with a slope proportional to the capacitor current slew rate. When the output of the accumulator equals

the calculated magnitude of the capacitor current  $|i_c(k_{end})|$ , it is determined that the capacitor current has crossed zero. If the ESR of the output capacitor is significant, a constant digital delay (of  $T_{del\_ESR} = C_o \cdot ESR$ ) may be added to the detection of  $t_1$  to compensate. In order to improve accuracy and mitigate quantization noise effects, each output voltage sample can be composed of a sum of successive output voltage samples acquired at a period  $1/2^x$  of  $T_{ic\_acq}$ .

Since the calculation of  $|m_{ic}|$  and  $|i_c(k_{end})|$  is unit-less and proportional to each other, the aforementioned method is capable of predicting the  $i_c$  zero cross-over point without knowledge of the input voltage, output voltage, nominal inductor value or the output voltage error sensor gain.

Immediately following the prediction of  $t_1$ , the controller will send a pulse to the *clr* input of *accumulator 1* to reset its output (as shown in Fig. 7-Fig. 9). The input of *accumulator 1* will then be set to  $kV_{in}$ .

If load-line regulation is enabled, the controller will also:

1. Sample the inductor current (by use of a RC network) for use in the linear compensator following the transient
2. Freeze the output of the *load-line accumulator*
3. Determine if Case #1 or Case #2 is occurring by comparing the output of *accumulator 2* with the output of the *load-line accumulator* (see Fig. 8-Fig. 9)

If Case #1 is detected or load-line regulation is not enabled, *accumulator 2* will be set to decrement (see Fig. 7-Fig. 8).

If Case #2 is detected, the converter's PWM signal will be set low (for a positive load step), as shown in Fig. 5. The *Case 2 Accumulator* will be activated and will increase linearly at a rate of  $kV_{in} \cdot 2 \cdot kV_o$ , as shown in Fig. 9.

### C. Step 3: Determine Switching Point $t_2$

If Case #1 is detected or load-line regulation is not enabled, the converter's PWM switch state will change at the moment that *accumulator 2*'s output is less than that of the *load-line accumulator* (see Fig. 7-Fig. 8). This will cause the inductor current  $i_L$  to slew toward the new load current  $I_{o2}$  (see Fig. 2-Fig. 4).

If Case #2 is detected, the *Case 2 accumulator* will begin to decrease linearly at a rate of  $kV_o$  (for a positive load step) when the output of *accumulator 2* exceeds that of the *load-line accumulator*. As shown in Fig. 9, when the *Case 2 accumulator* returns to zero,  $t_2$  is detected and the PWM state is altered. As shown in Fig. 5, the inductor current will begin to slew toward the new load current  $I_{o2}$ .

### D. Step 4: Determine End of Transient and Return Control to Linear Compensator

As illustrated in Fig. 2-Fig. 5, the end of the transient occurs when the inductor current  $i_L$  equals the new load current  $I_{o2}$  for a second instance at  $t_3$  (i.e. the moment that  $i_c$  equals zero for a second time). This can be detected by emulating the capacitor current following  $t_1$ . A digital

accumulator (*accumulator 3*) is used to emulate the magnitude of  $i_c$ . The accumulator increments during time interval  $T_1$  and decrements during time increment  $T_2$ . The input of *accumulator 3* is  $kV_{in}-kV_o$  when the converter's PWM signal is high and is  $kV_o$  when the output the PWM signal is low. In other words, the output of *accumulator 3* is proportional to the absolute value of the capacitor current  $i_c$  during  $T_1$  and  $T_2$ . Therefore, when the output of *accumulator 3* returns to zero,  $t_3$  is detected and transient is over.

When  $t_3$  is determined, the controller disables the transient controller and unfreezes the linear controller. It is important to note that the linear controller has already received the new load current  $I_{o2}$  (measured at  $t_1$ ) for load line regulation use. This operation will mitigate switchover effects that may occur following the transient-to-steady-state mode change.

### V. EXPERIMENTAL RESULTS

In order to demonstrate the proposed controller's effectiveness, a Buck converter prototype was built with the following parameters:  $V_{in}=12V$ ,  $V_o=1.5V$ ,  $f_{sw}=400kHz$ ,  $L_o=1\mu H$ ,  $C_o=180\mu F$ ,  $ESR=0.5m\Omega$ ,  $ESL=100pH$ . The output impedance  $R_{droop}$  was set to  $5m\Omega$ .

The voltage error ADC and the inductor current ADC each used 8-bit conversion; the ADC conversion range was 1V. The voltage error sensor gain  $G_{AD}$  was equal to 5.

The  $i_c$  zero cross-over predictor calculated the derivative every  $T_{ic\_acq}=160ns$  (from  $v_o$  samples acquired every 40ns) and was capable of producing an effective resolution of  $T_{ic\_clk}=10ns$ . The monitoring period of the  $i_c$  zero cross-over predictor was dynamic based on the direction of the load current transient. For positive load transients, the monitoring period was 320ns (i.e.  $N_{samp}=2$ ). For negative load transients, the monitoring period was 1.92us (i.e.  $N_{samp}=12$ ). It is important that the monitoring conclude before the inductor current equals  $I_{o2}$ .

The controller was implemented on an Altera Cyclone II FPGA chip. The chip is capable of utilizing over 70 000 logic elements; however, the combination of the  $i_c$  zero cross-over predictor and the double accumulator blocks only require a total of 450 logic elements. It is important to note that no multiplier, divider, square root or 2-dimensional LUTs were required to implement the digital charge balance controller.

The previously-defined converter and controller were subjected to rapid load current transients to demonstrate the effectiveness of the proposed controller. Fig. 12 illustrates the controller's reaction to a  $0A \rightarrow 11.5A$  load step (without load-line regulation). For reference, the time instants  $t_0-t_3$  were super-imposed on the scope display to better illustrate the controller's behavior.

Fig. 13 shows the controller's reaction to an  $11.5A \rightarrow 0A$  load step change (without load-line regulation).

Fig. 14 illustrates the controller's reaction to a  $0A \rightarrow 10A$  load step (with load line regulation).

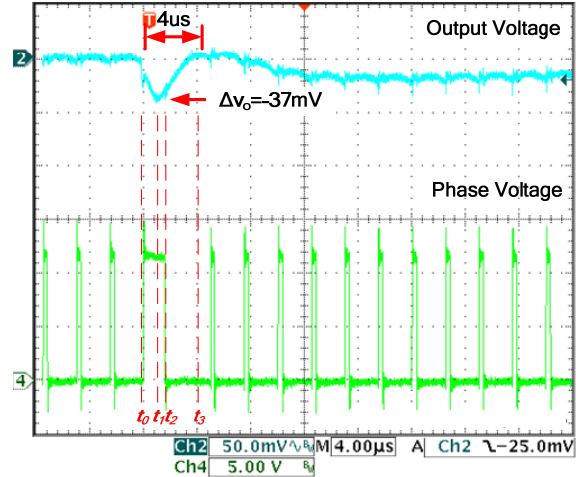


Fig. 12. Controller's response to  $0A \rightarrow 11.5A$  load step (w/o load line)

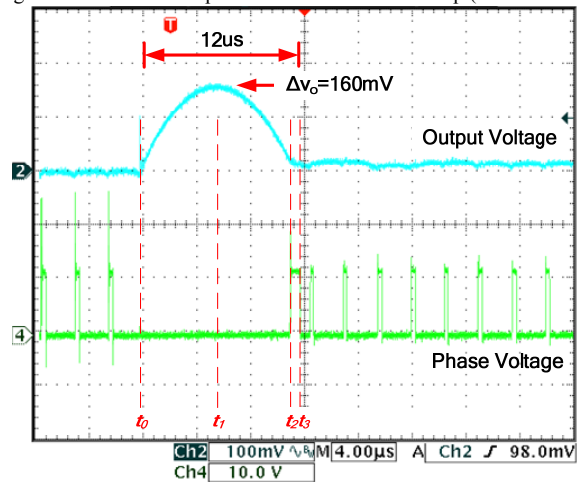


Fig. 13. Controller's response to a  $11.5A \rightarrow 0A$  load step (w/o load line)

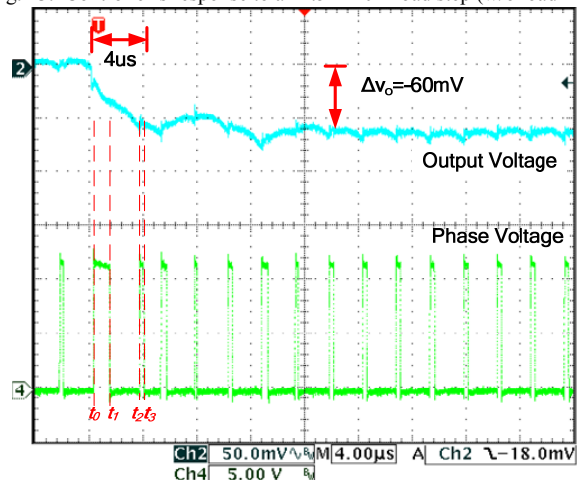


Fig. 14. Controller's response to a  $0A \rightarrow 11.5A$  load step (with load line)

As is observed in Fig. 14, Case #2 occurs for a  $0A \rightarrow 11.5A$  load step. As shown, the controller reacts to the positive load step by immediately setting the PWM signal high; however, when the inductor current equals the new load current (at  $t_1$ ), additional charge must be removed from output capacitor in order for the output voltage to decrease to its new steady-state

value. Thus, the PWM signal is set low until time instant  $t_2$  in order to remove additional charge from the output capacitor in the fastest manner possible.

For clearer understanding of the operation of the controller, the digital signals of the controller during the positive load current step transient are shown in Fig. 15. The digital signals were extracted during experimental tests using an embedded logic analyser. For reference, the time instants  $t_0-t_3$  were super-imposed on the graph.

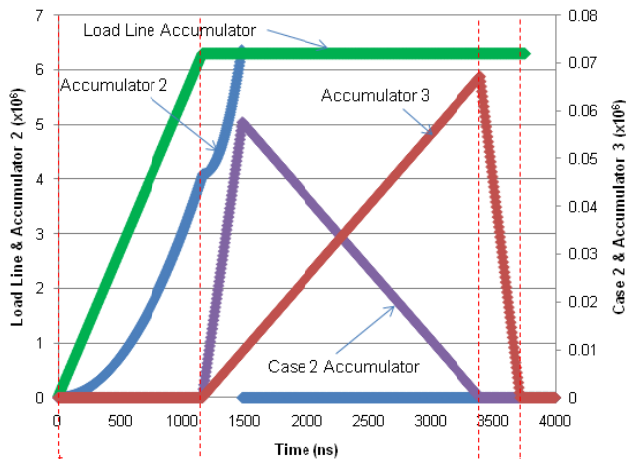


Fig. 15. Digital control signals of charge balance controller during 0A  $\rightarrow$  11.5A load current transient with load line-regulation (Case #2)

As illustrated, the controller is capable of detecting Case #2 at time instant  $t_1$ . If the load line accumulator output is greater than that of accumulator 2, additional charge must be removed from the capacitor and the condition for Case #2 exists. The case 2 accumulator is used to determine the switching moment  $t_2$ .

Fig. 16 illustrates the controller's reaction to an 11.5A  $\rightarrow$  0A load step (with load line regulation).

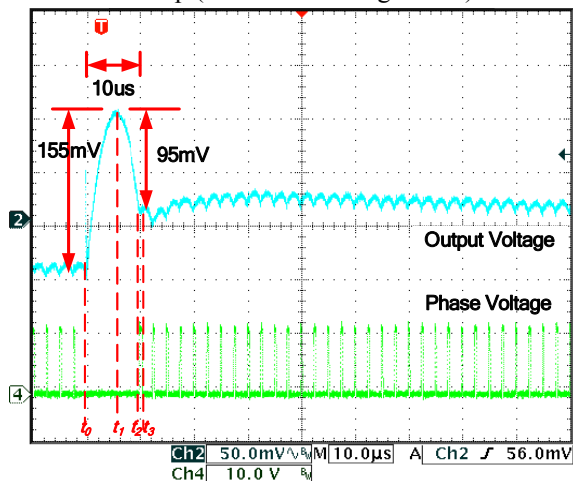


Fig. 16. Controller's response to a 11.5A  $\rightarrow$  0A load step (with load line)

It is shown that the transition between the charge balance controller and the linear controller is relatively smooth in Fig. 14 and Fig. 16. This is facilitated by the previously-measured load current information being passed to the linear controller.

## VI. CONCLUSION

A digitally-implemented charge balance controller was presented in this paper.

It is demonstrated that the proposed controller possesses the following advantages over previously-proposed controllers:

- 1) The proposed method uses an analog transient detector and an asynchronous "interrupt" in order to react to a load step virtually instantaneously, significantly improving the transient response,
- 2) The proposed controller does not require two-dimensional LUTs or multipliers to calculate optimal switching intervals, thereby decreasing the number of gates and chip real-estate required,
- 3) Unlike previous methods, the proposed controller does not require the nominal value of the output inductor to estimate the capacitor current zero cross-over point and calculate the appropriate switching intervals,
- 4) Through the addition of a couple of digital accumulators, the proposed method can be extended to load-line regulation applications, which is an important criteria in modern voltage regulators.

## VII. REFERENCES

- [1] K.K.S Leung, H.S.H. Chung, "Derivation of a Second-Order Switching Surface in the Boundary Control of Buck Converters", *IEEE Power Electronics Letters*, vol. 2, no. 2, June 2004, pp. 63-67
- [2] K.K.S Leung, H.S.H. Chung, "A Comparative Study of Boundary Control With First- and Second-Order Switching Surfaces for Buck Converters Operating in DCM", *IEEE Transactions on Power Electronics*, vol. 22, no. 4, July 2007, pp 1196-1209
- [3] E. Meyer, Z. Zhang, Y-F. Liu, "An Optimal Control Method for Buck Converters Using a Practical Capacitor Charge Balance Technique", *IEEE Transactions on Power Electronics*, vol. 23, no. 4, July 2008, pp. 1802-1812
- [4] A. Soto, A. de Castro, P. Alou, J.A. Cobos, J. Uceda, A. Lotfi, "Analysis of the Buck Converter for Scaling the Supply Voltage of Digital Circuits", *IEEE Transactions on Power Electronics*, vol. 22, no. 4, July 2007, pp. 1196-1209
- [5] S. Effler, A. Kelly, M. Halton, T. Kruger, K. Rinne, "Digital Control Law using a Novel Load Current Estimator Principle for Improved Transient Response", *IEEE Power Electronics Specialists Conference*, 2008, pp. 4585-4589
- [6] G. Feng, E. Meyer, Y.F. Liu, "A New Digital Control Algorithm to Achieve Optimal Dynamic Response Performance in DC-to-DC Converters", *IEEE Transactions on Power Electronics*, vol. 22, no. 4, July 2007, pp. 1489-1498
- [7] Z. Zhao, A. Prodic, "Continuous-Time Digital Controller for High-Frequency DC-DC Converters", *IEEE Transactions on Power Electronics*, vol. 23, no. 2 March 2008, pp. 564-573
- [8] V. Yousefzadeh, A. Babazadeh, B. Ramachandran, E. Alarcon, L. Pao, D. Maksimovic, "Proximate Time-Optimal Control for Synchronous Buck DC-DC Converters", *IEEE Transactions on Power Electronics*, vol. 23, no 4, July 2008, pp. 2018-2026
- [9] A. Costabeber, L. Corradini, P. Mattavelli, S. Saggini, "Time Optimal, Parameters-Insensitive Digital Controller for VRM Applications with Adaptive Voltage Positioning", *Control and Modeling for Power Electronics (COMPEL)*, 2008, pp. 1-8